

ANALYSIS AND CORRELATION OF FLUID MOTIONS IN NATURAL THERMAL CONVECTION IN A CYLINDRICAL VESSEL

by

Wei WANG*, **Xin-Lei GUAN**, **Li-Jun WANG**, and **Chu-Wen GUO**

School of Electrical and Power Engineering, China University of Mining and Technology,
Xuzhou, China

Original scientific paper
<https://doi.org/10.2298/TSC180605121W>

A natural thermal convection system is set up in a cylindrical vessel with aspect ratio of 2 having a temperature gradient in the vertical direction, and the fluid motions due to convection are investigated. The 2-D velocity field along the plane passing through the diameter of the vessel is obtained using particle image velocimetry. The results indicate that the convection is in the transition stage and the mean velocity fields show two pairs of counter-rotating circulations. The mean motions are predominant in the vertical direction under the influence of the temperature gradient, while the fluctuations in the x- and y-directions have the same order of magnitude. Probability density functions of fluctuation velocities at seven characteristic points show different behaviors. The space-time correlations in the regions where the circulations interact exhibit the iso-correlation-lines predicted by the elliptical approximation hypothesis. The space-time correlations of the streamwise and vertical fluctuations show distinct movements which imply the existence of anisotropy around the interaction region.

Key words: *natural-convection, large-scale circulation, space-time correlation, elliptical approximation*

Introduction

Natural thermal convections are a commonly observed and utilized phenomenon in industry. It is used for purposes such as the heat dissipation in heating pipes, and much effort has been spent on researching various aspects of this behavior [1, 2]. These studies have usually focused on theoretical questions in heat transfer, such as heat transport [3], geometrical dependency [4], and Prandtl number dependency [5]. In thermal convection, the temperature scalar is *passively* carried and transported by fluid elements, and hence, the investigation of fluid motions [6] can provide valuable information regarding the temperature transport. Researchers analyze the fluid motions via space-time correlations [7, 8] that provide ample information regarding the fluid behavior in both temporal and spatial dimensions. But the formulation of the space-time correlation requires high resolution in both dimensions, which is difficult to achieve even with state-of-the-art measurement techniques. Experimenters have to use the limited velocity information available to estimate space-time correlations. The classical method for the transformation from spatial or temporal correlation space-time correlation is the Taylor frozen hypothesis [9], expressed:

* Corresponding author, e-mail: wangwei@cumt.edu.cn

$$C(r, \tau) = C(r - \bar{U}\tau, 0) \quad (1)$$

where C is the correlation function normalized by the root mean square (RMS) value of the velocity fluctuation, r – the space separation, τ – the time delay, and \bar{U} – the local longitudinal mean velocity. The Taylor hypothesis has several defects, including its conflict with the fact that coherent motions must decay at large spatial or temporal separations. An advanced model for the space-time correlation, called the elliptic approximation (EA) hypothesis [10-12], was proposed and is represented:

$$C(r, \tau) = C\left\{\left[(r - U_c\tau)^2 + (V\tau)^2\right]^{1/2}, 0\right\} \quad (2)$$

where U_c is the convection velocity and V – the sweep velocity. The EA model gives better predictions for space-time correlations than the Taylor hypothesis and it has been validated by several experimental [13, 14] and numerical simulation studies [15-17]. The results obtained by Zhou *et al.* [18] agree well with the EA model in the case of Rayleigh-Benard convection. Hogg *et al.* [19] measured the density field of helium-sulfur hexafluoride mixtures using Schlieren method and found that the density scalar also obeyed the EA hypothesis. Wang *et al.* [20, 21] validated the EA model in a canonical turbulent boundary-layer using particle image velocimetry (PIV) data.

In this study, the 2-D velocity field that exists in a cylindrical container with a natural thermal convection system was obtained using PIV. The mean motions, fluctuations, and several dynamical characteristic points extracted from the flow were analyzed sequentially. Finally, the space-time correlations around the characteristic points were formulated and analyzed.

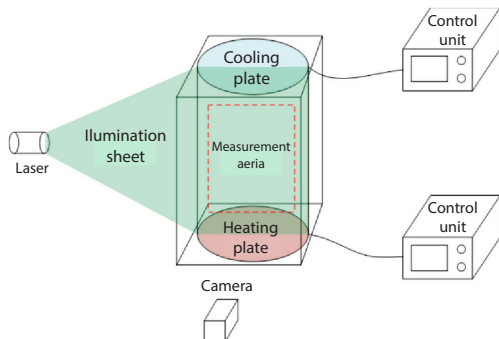


Figure 1. Experimental set-up

thermal convection became stable, the temperature at the top, T_t and temperature at the bottom T_b , measured by a thermocouple thermometer with an accuracy of ± 0.1 °C, were $T_b = 60.2$ °C and $T_t = 52.5$ °C, respectively. Fluid properties are determined in terms of the reference temperature $T_r = 1/2(T_b + T_t) = 56.4$ °C, resulting:

$$\text{Pr} = \frac{\mu c_p}{\lambda} = 3.26 \quad (3)$$

where Pr is the Prandtl number that denotes the ratio of the momentum diffusivity and the heat diffusivity, μ – the dynamic viscosity, c_p – the specific heat capacity, and λ – the thermal conductivity. The temperature difference $\Delta T \approx 8$ °C, giving:

$$\text{Gr} = \frac{g\alpha_v\Delta TH^3}{\nu^2} = 1.8 \cdot 10^{11} \quad (4)$$

Experimental set-up

The experiment was carried out in a small convection cell, shown in fig. 1. A cylindrical vessel made of borosilicate glass, with height $H = 157.5$ mm, the diameter $D = 76.5$ mm, resulting in an aspect ratio $\Gamma = H/D \approx 2$, was filled with pure water. A heating pad having an accuracy of ± 0.1 °C was placed below the glass vessel, separated from it by a layer of daubing thermal conductive silicone to enable heat conduction. A semiconductor-based refrigeration device was placed above the cell. When the

where Gr is the Grashof number that denotes the ratio of the buoyancy force and the viscous force, g – the gravitational acceleration, α_V – the volumetric expansion coefficient, and ν – the kinetic viscosity.

$$Ra = Gr \cdot Pr = 5.8 \cdot 10^{11} \quad (5)$$

where Ra is the Rayleigh number. Grashof number, rather than Rayleigh number, is recommended as the criterion that determines the flow state in a convective flow [22].

A Dantec PIV system was used for the acquisition of the velocity field in the convective flow. A series of 10800 snapshots of a plane through the diameter was collected with sampling rate 10 Hz. After cross-correlating the particle images, a measurement area of $70 \times 150 \text{ mm}^2$ produced $57 \times 120 = 6840$ velocity vectors with a vector separation of 1.2657 mm in both x - and y - directions.

Results and discussions

Figures 2(a)-2(d) show the distributions of the streamwise mean velocity, \bar{U} , wall-normal mean velocity, \bar{V} , velocity magnitude, and streamlines, respectively. The signs of \bar{U} and \bar{V} change along the x -direction from fig. 2(a) and 2(b) considering that the temperature variation ΔT is along the y -direction, fig. 2(b) revealed that the heating fluid moves upward along the right side, while the cooling fluid moves downward along the left side. Figure 2(c) is the magnitude of the velocity $|\bar{V}| = (\bar{U}^2 + \bar{V}^2)^{1/2}$. For mean motions, the vertical motion is more dominant than the streamwise motion. In fig. 2(d), there exist two half H circulations instead of one large-scale circulation, which is a characteristic feature of turbulent convection. The two circulations whose centers are labeled as C and E are counterclockwise. In the top-right and lower-left corners, two clockwise small-scale circulations A and G are formed owing to the vorticity conservation. The label D denotes the saddle point created by the impact of the two circulations C and E. Points B and F are taken from the confluences in the upper and lower regions, respectively.

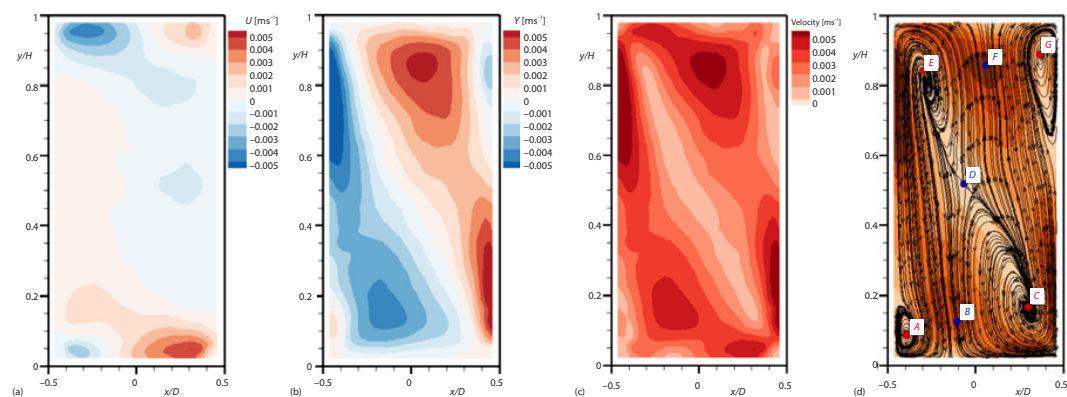


Figure 2. (a) Distribution of streamwise mean velocity, (b) distribution of wall-normal mean velocity, (c) distribution of velocity magnitude, and (d) streamlines indicate the mean flow and labels A-G denote seven characteristic points (for color image see journal web site)

The turbulent intensity is a quantity that represents the predominance of fluctuating motion with respect to the mean motions:

$$\sigma_u = \frac{(\overline{u'^2})^{1/2}}{\bar{U}}, \quad \sigma_v = \frac{(\overline{v'^2})^{1/2}}{\bar{V}} \quad (6)$$

where u' and v' are, the streamwise and vertical fluctuation velocities, respectively. Figure 3(a) and 3(b) have three characteristics;

- the magnitudes of σ_u and σ_v are equal, which implies that the fluctuated motions are nearly isotropic,
- the σ_u and σ_v are usually $\sim 0(10)$ in the bulk, which indicates that the velocity of fluctuation is of the same order of magnitude as the mean velocity, emphasizing the importance of small-scale fluctuations in natural-convection, and
- the high values of σ_u and σ_v reduce greatly along the zero lines of corresponding mean velocities, respectively. In fig. 3(c) the high kinetic energy values k are observed along the sidewall, which suggests that k stem from the confluence of the counter-rotating pairs of circulations. The Reynolds stress represents the exchange of momentum components in different directions. From fig. 3(d) it is seen that the extreme of the Reynolds stress occur in the vicinity of the heating and cooling boundaries, which is associated with the existence of instantaneous coherent structures or *thermal plumes* [1, 3]. Momentum and energy are exchanged by the plumes, transported across the central region of the cell by the circulations, and interact with the corresponding flows from the other side of the cell.

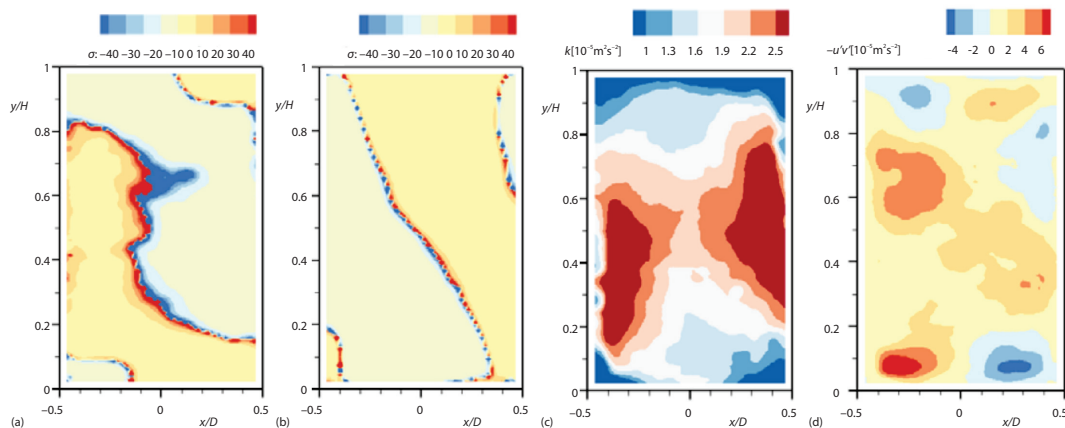


Figure 3. Distribution of (a) streamwise turbulent intensity, (b) wall-normal turbulent intensity, (c) kinetic energy, and (d) Reynolds stress $-\overline{u'v'}$ (for color image see journal web site)

The probability density function (PDF), which is a statistical quantity, corresponding to seven characteristic points has been extracted. The PDF reveal the skewness and concentration of the fluctuations. Points A, C, E, and G at centers of the circulations in fig. 4(a) and points B, D, and F at the interaction regions in fig. 4(b) show a similar tendency for PDF of u' . The PDF showed a clear disparity between the points in the center and those in the interaction region in fig. 4(c). The points in the center have higher PDF values for lower u' in the vicinity of the zero fluctuation, meanwhile the latter has PDF values for higher u' and lower peaks in the vicinity of the zero. For the PDF of v' in fig. 4(d), it is shown that skewness of the PDF are related to the locations of the center: in the lower location C, v' tends to be positive, whereas it tends to be negative in the upper location E. The PDF at points B, D, and F are nearly identical. In fig. 4(f), it is seen that PDF of v' between the center and the interaction region have more distinct peaks compared to those associated with u' .

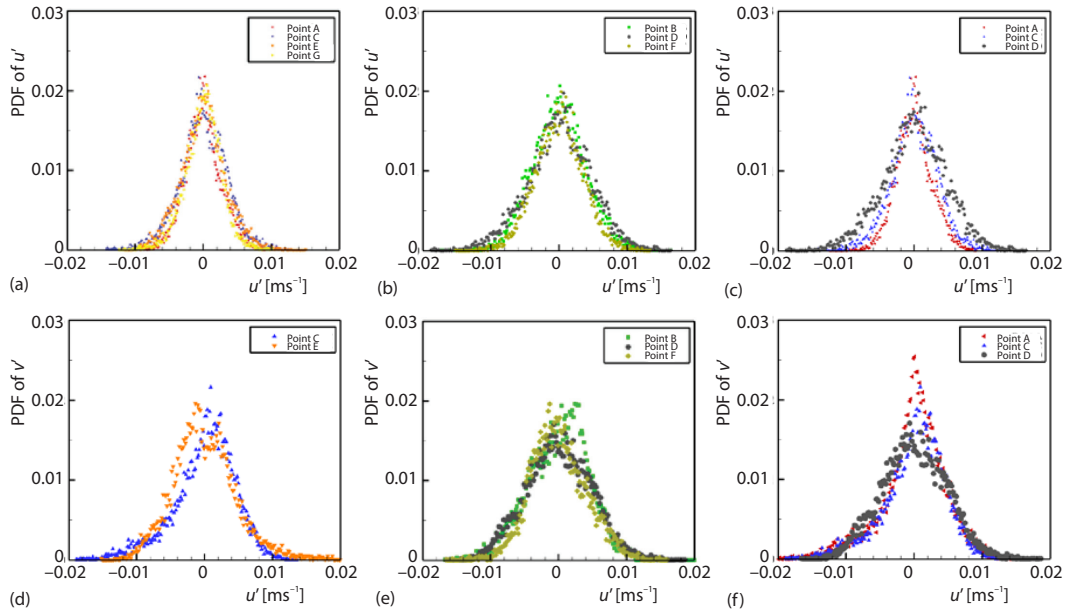


Figure 4. The PDF of u' at (a) points A, C, E, and G, (b) points B, D, and F, (c) points A, C, and D, PDF of v' at (d) points C and E, (e) points B, D, and F, and (f) points A, C, and D

The space-time correlations of the velocity field are calculated based on eqs. (7)-(10):

$$C_{uu}(r_x, \tau) = \frac{\overline{u'(r, t)u'(r + r_x, t + \tau)}}{u_{\text{rms}}(r)u_{\text{rms}}(r + r_x)} \quad (7)$$

$$C_{uu}(r_y, \tau) = \frac{\overline{u'(r, t)u'(r + r_y, t + \tau)}}{u_{\text{rms}}(r)u_{\text{rms}}(r + r_y)} \quad (8)$$

$$C_{vv}(r_x, \tau) = \frac{\overline{v'(r, t)v'(r + r_x, t + \tau)}}{v_{\text{rms}}(r)v_{\text{rms}}(r + r_x)} \quad (9)$$

$$C_{vv}(r_y, \tau) = \frac{\overline{v'(r, t)v'(r + r_y, t + \tau)}}{v_{\text{rms}}(r)v_{\text{rms}}(r + r_y)} \quad (10)$$

where C_{uu} and C_{vv} are normalized space-time correlations for u' and v' are the streamwise and vertical separations, respectively, u_{rms} and v_{rms} – the RMS of u' and v' . Figures 5(a)-5(d) show the space-time correlations in the vicinity of the saddle point D. The four space-time correlations all exhibit elliptical curves of iso-correlation which bolster the validity of EA hypothesis in the case of natural thermal convection. In addition the elliptical shape of the space-time correlations, it is revealed that u' and v' have distinct characteristics for the correlations in the x - and y - directions. The EA hypothesis states that the preferred direction of the elliptical curves depends on the convective motion of the coherent structure. The results shown in fig. 5 imply differences in the movements of u' - u' and v' - v' coherent structures in the x - and y -directions. It is suggested that the fluid motion in the region of interaction of the circulations is anisotropic

in contrast to large-scale circulation which can effectively approximated as a homogeneous isotropic turbulence. It is noted that the turbulence model for the former should be carefully discriminated from the model for the latter.

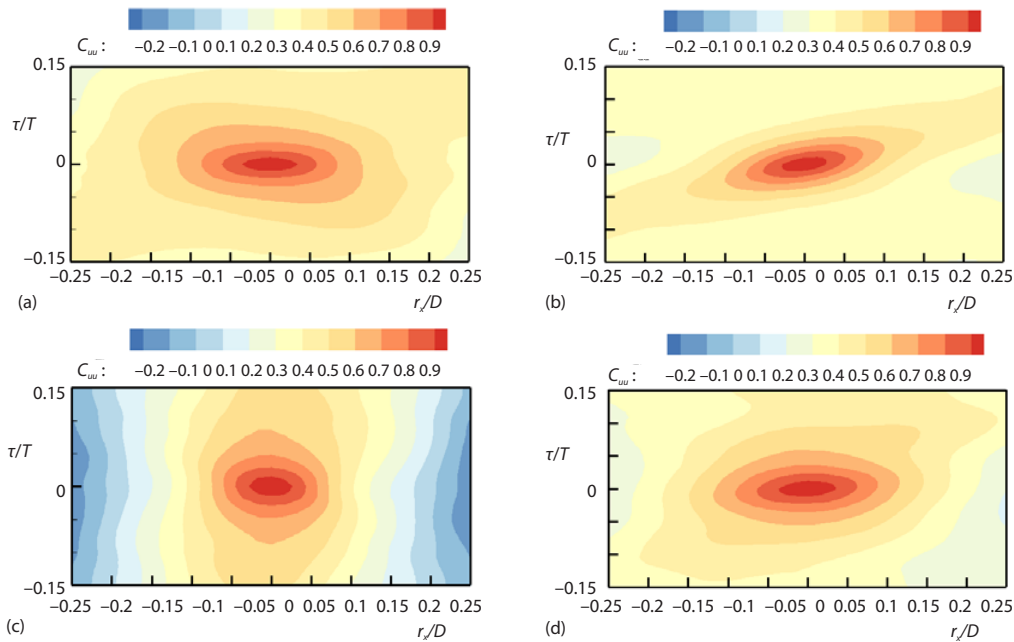


Figure 5. Space-time correlations of C_{uu} with respect to (a) r_x , (b) r_y , and C_{vv} with respect to (c) r_x and (d) r_y .

Conclusion

In this study, a natural thermal convection system was established and relevant quantities were measured using PIV. The 2-D velocity field was analyzed in terms of the mean motions, fluctuations, and space-time correlations. The obtained mean velocity fields show that the convection is in the transition stage and the system has two pairs of counter-rotating circulations. As a result of the temperature gradient in the vertical direction, the mean motion in the direction normal to the wall is stronger than the streamwise mean motion. In contrast, the fluctuations along the x - and y -directions have the same order of magnitude, which bring to the fore the distinct characteristics of the mean motion and fluctuating motion. For the different dynamic characteristic points considered, the concentration, and skewness of the fluctuation velocities show differences. Space-time correlations at the region of interaction of the circulations obey the EA hypothesis, but reveal the anisotropy of the streamwise and vertical fluctuating motions.

Acknowledgment

This work was supported by the Fundamental Research Funds for the Central Universities (Grant No. 2017XKZD02) and the National Natural Science Foundation of China (Grant No. 11802331).

Nomenclature

c_p – specific heat capacity, [$\text{Jkg}^{-1}\text{C}^{-1}$]
 D – diameter, [m]
 g – gravitational acceleration, [ms^{-2}]

H – height, [m]
 r – space separation, [m]
 ΔT – temperature difference, [$^{\circ}\text{C}$]

T_b – bottom temperature, [°C]
 T_t – top temperature, [°C]
 U_c – convection velocity, [ms⁻¹]
 V – sweep velocity, [m/s]

Greek symbols

α_V – volumetric expansion coefficient, [1°C⁻¹]
 λ – thermal conductivity, [Wm⁻¹K⁻¹]
 μ – dynamical viscosity, [kgm⁻¹s⁻¹]
 ν – kinetic viscosity, [m²s⁻¹]
 σ_u – streamwise turbulent intensity
 σ_v – wall normal turbulent intensity
 τ – time delay, [s]

References

- [1] Ahlers, G., Turbulent Convection. *Physics*, 2 (2009), 74, pp. 1-7
- [2] He, X., et al., Transition the Ultimate State of Turbulent Rayleigh-Bénard Convection, *Physical Review Letters*, 108 (2013), 2, 014503
- [3] Chong, K., et al., Effect of Prandtl Number on Heat Transport Enhancement in Rayleigh-Benard Convection Under Geometrical Confinement, *Physical Review Fluids*, 3 (2018), 1, 013501
- [4] Kaczorowski, M., et al., Turbulent Flow in the Bulk of Rayleigh-Benard Convection: Aspect-Ratio Dependence of the Small-Scale Properties, *Journal of Fluid Mechanics*, 722 (2013), 5, pp. 596-617
- [5] Ni, R., et al., Reversals of the Large-Scale Circulation in Quasi-2D Rayleigh-Bénard Convection, *Journal of Fluid Mechanics*, 778 (2015), R5, pp. 1-11
- [6] Xi, H., et al., Higher-Order Flow Modes in Turbulent Rayleigh-Benard Convection, *Journal of Fluid Mechanics*, 805 (2016), Oct., pp. 31-51
- [7] He, X., et al., Logarithmic Spatial Variations and Universal f^{-1} Powerspectra of Temperature Fluctuations in Turbulent Rayleigh-Benard Convection, *Physical Review Letters*, 112 (2014), 17, 174501
- [8] He, X., et al., Reynolds Numbers and the Elliptic Approximation Near the Ultimate State of Turbulent Rayleigh-Benard Convection, *New Journal of Physics*, 17 (2015), June, 063028
- [9] Taylor, G., The Spectrum of Turbulence, *Proceedings of the Royal Society of London A: Mathematical, Physical and Engineering Sciences*, London, England, 1938, Vol. 919, pp. 476-490
- [10] He, G., et al., On the Computation of Space-Time Correlations by Large-Eddy Simulation. *Physics of Fluids*, 11 (2003), 16, pp. 319-330
- [11] He, G., et al., Elliptic Model for Space-Time Correlations in Turbulent Shear Flows. *Physical Review E*, 73 (2006), 5, 055303
- [12] Zhao, X., et al., Space-Time Correlations of Fluctuating Velocities in Turbulent Shear Flows. *Physical Review E*, 79 (2009), Apr., 046316
- [13] He, X., et al., Small-Scale Turbulent Fluctuations Beyond Taylor's Frozen-Flow Hypothesis, *Physical Review E*, 81 (2010), 6, 065303
- [14] Guo, L., et al., The LES Prediction of Space-Time Correlations in Turbulent Shear Flows, *Acta Mechanica Sinica*, 4 (2012), 28, pp. 993-998
- [15] Wallace, J., Space-Time Correlations in Turbulent Flow: A Review, *Theoretical & Applied Mechanics Letters*, 2 (2014), 4, 4022003
- [16] Geng, C., et al., Taylor's Hypothesis in Turbulent Channel Flow Considered Using a Transport Equation Analysis, *Physics of Fluids*, 27 (2015), 2, 025111
- [17] He, G., et al., Space-Time Correlations and Dynamic Coupling in Turbulent Flows. *Annual Review of Fluid Mechanics*, 1 (2017), 49, pp. 51-70
- [18] Zhou, Q., et al., Experimental Investigation of Longitudinal Space-Time Correlations of the Velocity Field in Turbulent Rayleigh-Benard Convection, *Journal of Fluid Mechanics*, 3 (2011), 683, pp. 94-111
- [19] Hogg, J., et al., Reynolds-Number Measurements for Low-Prandtl-Number Turbulent Convection of Large-Aspect-Ratio Samples. *Journal of Fluid Mechanics*, 5 (2013), 725, pp. 664-680
- [20] Wang, W., et al., The TRPIV Investigation of Space-Time Correlation in Turbulent Flows over Flat and Wavy Walls. *Acta Mechanica Sinica*, 4 (2014), 30, pp. 468-479
- [21] Wang, W., et al., Convection and Correlation of Coherent Structure in Turbulent Boundary-Layer Using Tomographic Particle Image Velocimetry, *Chinese Physics B*, 10 (2014), 23, pp. 323-333
- [22] Yang, S., et al., *Heat Transfer* (in Chinese), Higher Education Press, Beijing, 2006